Cement & Concrete Composites 34 (2012) 835–847

Contents lists available at SciVerse ScienceDirect

Cement & Concrete Composites

journal homepage: www.elsevier.com/locate/cemconcomp

Increasing the reactivity of metakaolin-cement blends using zinc oxide

Sarah C. Taylor-Lange [a,*], Kyle A. Riding [b], Maria C.G. Juenger [a]

[a] *Department of Civil, Architectural, and Environmental Engineering, 1 University Station C1748, The University of Texas at Austin, Austin, TX 78712, USA*
[b] *Department of Civil Engineering, 2107 Fiedler Hall, Kansas State University, Manhattan, KS 66506, USA*

ARTICLE INFO

Article history:
Received 12 July 2011
Received in revised form 3 March 2012
Accepted 7 March 2012
Available online 17 March 2012

Keywords:
Metakaolin
Kaolinite
Supplementary cementitious materials
Zinc oxide
Dehydroxylation
Pozzolan

ABSTRACT

This study aimed to improve the reactivity of metakaolin-cement mixtures using ZnO additions. Kaolinite samples with 0.1–1 wt% ZnO were calcined at temperature intervals of 50 °C from 500 to 650 °C for 1 h. The resulting metakaolins were examined for structural changes after calcination and for their pozzolanic reactivity, influence on the hydration behavior of cement pastes, and impact on the compressive strength of mortar cubes. ZnO behaved as a delayed accelerator for cement paste. However, when ZnO was combined with highly amorphous metakaolin, chemical retardation was eliminated while acceleration was maintained. Such systems also had increased 28-day compressive strengths. ZnO additions did not affect the degree of dehydroxylation or the pozzolanic reactivity of the metakaolin. These results could facilitate the use of less pure calcined clays as SCM by providing a mechanism for improving reactivity and may also impact the ability to use zinc-contaminated materials in concrete.

© 2012 Elsevier Ltd. All rights reserved.

1. Introduction

The most commonly used calcined clay as a supplementary cementitious material (SCM) is calcined kaolinite, called metakaolin. Using metakaolin as a partial substitute for Portland cement in concrete has been shown to increase long-term strength and durability compared with Portland cement alone and reduce the quantity of cement required, thereby lowering concrete carbon dioxide footprint associated with cement manufacturing [1–3]. Kaolinite is classified as a 1:1 clay mineral, consisting of one tetrahedral sheet and one octahedral sheet held together by weak van de Waals forces [4]. Ground kaolinite [$Al_2Si_2O_5(OH)_4$], which is theoretically composed of 46.54% SiO_2, 39.50% Al_2O_3 and 13.96% H_2O, forms metakaolin [$Al_2Si_2O_7$] through the loss of the lattice oxygen and hydroxyl groups following heat treatment at 500–800 °C [5,6]. During the most active period of cement hydration, from 3 h to 24 h, cement reacts to form C–S–H,[1] calcium hydroxide, and ettringite, yet metakaolin is relatively inert [7]. The amorphous metakaolin pozzolanically reacts with the $Ca(OH)_2$ formed from cement hydration forming (i) C–S–H gel, (ii) crystalline calcium aluminate hydrates [C_4AH_{13}, C_3AH_6], and (iii) crystalline calcium aluminosilicate [C_2ASH_8] [7–10]. Generally, metakaolin has a positive effect on concrete strength following 48 h of hydration, increasing strength relative to neat cement systems due to the pozzolanic reactivity [8].

It was of interest in this study to improve the reactivity of metakaolin-cement mixtures. Influencing the reactivity of an SCM-cement blend can be achieved by either (1) increasing early cement hydration to compensate for the dilution effect of the SCM and/or (2) enhancing the pozzolanic reactivity of the SCM. The idea in this case was to enhance the reactivity of metakaolin-cement blends to enable the use of calcined impure, kaolin-containing clays as SCMs. Calcined impure clays have a lower reactivity compared to pure metakaolin [6,9], however they are desirable as SCMs due to higher availability and lower cost compared to pure kaolinite. Enabling the use of impure clays, by compensating for the lower reactivity may facilitate their use as SCMs.

Some limited research has been conducted on altering kaolinite mineralogical properties, in turn potentially changing the reactivity of the SCM [11–14]. San Cristóbal et al. [11] pretreated kaolinite with 6 M HCl at 90 °C for 3 h, followed by centrifugation at 10,000 rpm, and then calcination; they found that the acid substantially altered the physico-chemical, mineralogical and morphological properties of the metakaolin. However, San Cristóbal et al. [11] did not test the effects of this treated kaolinite on pozzolanic reactivity. Similarly, Lenarda et al. [12] treated kaolinite with 1 M H_2SO_4 at 90 °C, followed by calcination at 850 °C, resulting in metakaolins with a high surface area and good catalytic properties. Kuechler [13] used cone fusion to demonstrate that the addition of titanium dioxide and iron oxide prior to calcination lowered the refractoriness of calcined kaolinite (i.e. thermal resistance). Chatterji et al. [14] demonstrated that the addition of 0.001 wt%,

---

* Corresponding author. Tel.: +1 310 499 3924; fax: +1 512 471 4555.
E-mail address: staylorla@gmail.com (S.C. Taylor-Lange).

[1] Cement chemistry notation is used throughout, whereby single letters represent oxides: A = Al_2O_3, C = CaO, F = Fe_2O_3, H = H_2O, S = SiO_2, and $\hat{S}$ = SO_3. The dashes in "C–S–H" indicate variable stoichiometry.

0958-9465/$ - see front matter © 2012 Elsevier Ltd. All rights reserved.
http://dx.doi.org/10.1016/j.cemconcomp.2012.03.004

0.01 wt% and 0.1 wt% zinc oxide increased the pozzolanic reactivity of kaolinite measured by lime reactivity tests. In addition, Chatterji et al. [14] measured the compressive strength of ZnO-metakaolin-hydrated lime mixtures and saw an approximately 50% increase in compressive strength compared to mixtures with no zinc oxide. The work by Chatterji et al. [14] provided the groundwork for this study, which investigated the use of ZnO to change the reactivity of metakaolin.

Chatterji et al. [14] investigated blends of metakaolin and lime, rather than Portland cement. The addition of zinc and zinc oxide to Portland cement has been shown to (i) greatly retard hydration, increasing the induction periods from hours to weeks, (ii) alter the rate of heat evolution, and (iii) reduce compressive strength [15]. For example, the waste material electric arc furnace dust (EAFD), which contains from 10 wt% to 90 wt% zinc depending upon processing, has been shown to consistently retard setting time when used in concrete mixtures [16]. Al-Zaid et al. [16] concluded that EAFD dust with 10 wt% zinc can be used as a retarding admixture, complying with the ASTM C494 standard. Puertas et al. [17] made cement clinker with ceramic waste which contained 0.02–0.12 wt% zinc oxide and demonstrated that this clinker exhibited longer initial and final setting time by 37 min and 70 min, respectively, compared with ordinary clinker. In addition, zinc-containing materials have been shown to affect the hydration of non-Portland cement binders, including calcium sulfoaluminate cements [17] and calcium aluminate cements [18], in both cases retarding hydration.

In this study, the ZnO was added to kaolinite prior to calcination because it was speculated that ZnO might be adsorbed by the kaolinite, modifying the structure of the metakaolin and enhancing its reactivity. The adsorption of heavy metal ions (Cu, Pb, Cd, Zn) by modified kaolinite minerals has been extensively studied in soil remediation and wastewater treatment [4,19–25]. Sajidu et al. [4] demonstrated that Zn(II) species were sorbed and hydrolysed on alkaline impure clay surfaces containing a low ordered kaolinite. Amer et al. [25] showed that the adsorption of metal ions onto a clay mineral substrate had both a positive enthalpy and entropy, implying an energetically favorable interaction. Additionally, both Farrah and Pickering [19] and Amer et al. [25] showed that the uptake of divalent cations by kaolinite increased as a function of increasing pH. Surfaces of kaolinite onto which metal adsorption can occur include: (1) the hydroxyl plane associated with the alumina octahedral layer, (2) the oxygen plane on the silica tetrahedral layer and, (3) particle edges from incomplete or irregular lattice structure [4].

The goal of the study was to investigate the ability of ZnO to improve the reactivity of metakaolin. The calcination temperature of kaolinite and wt% ZnO addition were varied to determine the minimum calcination temperature for complete dehydroxylation of kaolinite in the presence and absence of ZnO. The effects of the resulting metakaolins on early hydration rate of cement pastes and compressive strength of cement mortars were measured. The pozzolanic reactivity of the metakaolins was also measured. The results from this study may allow for the potential offsetting of the non-reactive portion of other clay minerals in an impure calcined clay SCM system. Moreover, enabling the use of ZnO in concrete opens the door to a variety of zinc or ZnO-containing waste materials that could then be used as concrete additives, such as electric arc furnace dust (EAFD).

2. Materials and methods

2.1. Materials

The primary materials used in this study included (i) zinc oxide (ZnO) (Acrōs Organics, 99%), (ii) ground kaolinite [$Al_2Si_2O_5(OH)_4$] (Wards Natural Science Establishment, Inc.), (iii) Two ASTM C150 [26] Type I Portland cement (Texas Lehigh Cement Co.) with Cement A processed in June 2009 and Cement B processed November 2011, (iv) ASTM C109 [27] Ottawa Silica Sand (Humboldt) and, (v) deionized water. The chemical composition of the Portland cements are shown in Table 1. The average particle diameter (d_{50}) was experimentally determined using laser diffraction (Fritsch Analysette 22) for ZnO and kaolinite materials. The average particle diameter (d_{50}) for ZnO was 1.4 μm and for kaolinite was 5.3 μm (Fig. 1). An effort was made to have a similar particle diameter (1–6 μm) to reduce the possibility of the ZnO greatly influencing kaolinite calcination or cement hydration due to particle size. The particle size of metakaolin (kaolinite calcined to 550 °C for 1 h) was also tested, showing the greatest average particle diameter (d_{50} = 6.5 μm), possibly due to clumping during the firing process (Fig. 1). For comparison, the typical industry standard size for metakaolin commercially produced for use as an SCM is 1–2 μm and for Type I Portland cement is 10–15 μm [29]. The cement Blaine fineness (ASTM C204) was tested experimentally using an air permeability apparatus (Humboldt), resulting in an average of 436 m^2/kg (based on triplicate tests) for Cement A and 386 m^2/kg for Cement B [28]. The sieve gradation for the ASTM C109 Ottawa sand, provided by the manufacturer is as follows: 98% retained on sieve No. 100 (150 μm), 75% retained on sieve No. 50 (300 μm), 30% retained on sieve No. 40 (425 μm) and, 2% retained on sieve No. 30 (600 μm). All the materials used in this study fall within the typical industry standard ranges.

2.2. Calcination

Zinc oxide was added in quantities of 0.1 wt%, 0.5 wt% and 1.0 wt% to 5 g of ground kaolinite and mixed by hand for 2 min prior to thermal activation. Metakaolin control samples contained no ZnO addition. Four calcination temperatures of 500 °C, 550 °C, 600 °C, and 650 °C were selected. The calcination protocol included (i) increasing the temperature from the ambient temperature to the specific calcination temperature at a rate of 25 °C/min, (ii) maintaining the specific calcination temperature for 1 h and, (iii) slow cooling to ambient temperature (i.e. specimens remained in the furnace until the furnace temperature reached ambient). The upper temperature limit for calcination was chosen according to Bich et al. [30] who demonstrated the difference in dehydroxylated content for metakaolins calcined at 650 °C, 700 °C and 800 °C was minimal to none, depending upon on the mineralogical composition of the kaolinite sample. In addition, higher temperatures were not selected since higher energy used for dehydroxylation could offset the environmental benefits of using calcined clays as substitutes for Portland cement. Three separate batches were fabricated and fired independently in an electric furnace (Lindberg Blue M).

Table 1
Oxide content of Type I Portland cement from Texas Lehigh.

Oxide	Cement A composition (%)	Cement B composition (%)
SiO_2	19.69	19.36
$A1_2O_3$	5.52	5.13
Fe_2O_3	2.49	2.53
CaO	63.06	63.17
MgO	1.16	1.03
SO_3	3.38	3.22
Na_2O	0.77	0.086
K_2O	0.97	0.88
TiO_2	0.25	0.23
SrO	NA	0.08
Mn_2O_3	NA	0.042
P2O5	0.29	0.22
Cl	NA	0.009
ZnO	NA	0.0071
Cr_2O_3	NA	0.0104

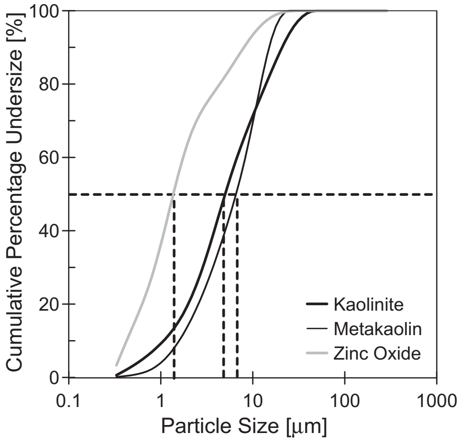

Fig. 1. Cumulative percentage undersize (%) vs. particle size (µm) of kaolinite, kaolinite heat treated.

Table 2 shows the experimental matrix, highlighting the wt% ZnO additions, calcination temperature, and the experimental tests conducted.

2.3. Degree of dehydroxylation

Thermal activation changes the crystalline nature of kaolinite to an amorphous metakaolin phase by dehydroxylation, the partial break down or loss of lattice hydroxyl groups [3,30]. The degree of dehydroxylation and associated mass loss due to evaporation of hydroxyl groups was determined by differential scanning calorimetry (DSC) and thermogravimetric analysis (TGA) using a differential thermal analyzer (NETZSCH STA 409). Samples were tested in platinum crucibles under a nitrogen atmosphere with a scanning rate of 10 °C/min from 25 °C to 1000 °C. Results were analyzed using Proteus Thermal Analysis software.

An approximate quantification of the percent dehydroxylation after calcination was determined by using the endothermic peak area acquired from DSC data. The peak area was calculated using Proteus Thermal Analysis software, with a linear baseline assumption. The area was integrated over a standard time range for all curves evaluated. Per Eq. (1), the peak area of a non-calcined sample (i.e. no-dehydroxylation) was compared to the peak area of a calcined sample (i.e. some dehydroxylation) [30]:

$$D(\%) = \frac{SK - SMK}{SK} * 100 \qquad (1)$$

where $D(\%)$ is the degree of dehydroxylation, SK is the area of the endothermic peak corresponding to kaolinite dehydroxylation and SKM is the area of the residual peak of remaining kaolinite in the metakaolin. Sixty percent of the samples were tested in duplicate to determine an approximate sample error.

The kaolinite crystalline composition was quantified using X-ray diffraction (XRD) analysis. XRD scans used Cu Kα radiation over a scan range of 10–50° 2θ in increments of 0.02° 2θ (Siemens Diffraktometer). XRD results were analyzed using Jade analysis software. Duplicate scans were conducted to give an approximate error for sample peak intensity.

^{29}Si and ^{27}Al MAS NMR were tested to examine differences between metakaolin with 1 wt% ZnO additions added prior to calcination (650 °C for 1 h.) compared with non-ZnO containing metakaolin subjected to the same heating cycle. ^{29}Si and ^{27}Al MAS NMR experiments were performed with a Bruker Avance-400 spectrometer equipped with a standard 7-mm MAS probe head. Samples were finely ground (passing 45 µm sieve) and tightly packed into a high-speed spinning NMR tube. Signals of ^{29}Si and ^{27}Al MAS NMR were recorded at a spinning rate of 7 kHz. ^{29}Si and ^{27}Al chemical shifts were referred to external tetramethylsilane (TMS) and an $AlCl_3$ solution, respectively.

2.4. Hydration

The rate of heat evolution (J/h/g) and the cumulative heat evolved (J/g) of ZnO-metakaolin-cement pastes were experimentally determined using an eight-channel isothermal calorimeter (TA Instruments TAM Air) following ASTM C1702-*Method B* [31]. Kaolinite with 0 wt%, 0.1 wt%, 0.5 wt% and 1.0 wt% ZnO additions and calcined at each prescribed temperature (500 °C, 550 °C, 600 °C, and 650 °C) replaced Portland cement in the pastes at levels of 0 wt% and 15 wt%.

Table 2
The experimental matrix, showing the calcination temperature and wt% of ZnO additions selected for the metakaolin preparatory treatment and the experimental test conducted.

Sample	DSC and TGA	XRD (kaolinite)	^{29}Si and ^{27}Al MAS NMR	Isothermal calorimetry	XRD (21 h)	Chapelle test	XRD (7 and 28 day)	Compressive strength
Uncalcined temperature 23 °C								
No ZnO	x	x						
0.l wt%ZnO								
0.5 wt%ZnO	x	x						
1.0 wt%ZnO	x	x						
Calcination temperature 500 °C								
No ZnO	x	x		x		x	x	x
0.l wt%ZnO				x				
0.5 wt%ZnO	x	x		x				
1.0 wt%ZnO	x	x		x	x	x	x	x
Calcination temperature 550 °C and 600 °C								
No ZnO	x	x		x				x
0.l wt%ZnO				x				
0.5 wt%ZnO	x	x		x				
1.0 wt%ZnO	x	x		x	x			x
Calcination temperature 650 °C								
No ZnO	x	x	x	x		x	x	x
0.l wt%ZnO				x				
0.5 wt%ZnO	x	x		x				
1.0 wt%ZnO	x	x	x	x	x	x	x	x

Letter ‘x’ indicates the sample was tested.

Metakaolin-cement pastes had a water-to-cementitious material ratio of 0.4 by mass and were mixed by hand for 2 min. After mixing, 10 g of paste was placed into a glass sample vial. A deionized water reference sample was used with a volume calculated to match the specific heat capacity of the metakaolin-cement paste (per Eq. (2)) [32].

$$c_p = \frac{c_c \cdot m_c + c_m \cdot m_m + c_w \cdot v_w}{m_p} \tag{2}$$

where c_c, c_m, c_w, and c_p are the specific heat capacity of the cement, metakaolin, water and paste (J/g K), respectively; m_c, m_m, and m_p are the mass of the metakaolin, cement, and paste (g), respectively; and v_w is the volume of water used in the cement paste sample (ml). The specific heat capacities of cement, water and kaolinite at 25 °C were approximated to be 0.75 J/(g K), 4.18 J/(g K), and 0.945 J/(g K) respectively [33–35]. Any variations in the specific heat capacity due to calcination temperature range (500–650 °C) were assumed to be negligible and were not taken into account when calculating the mass of the reference water for the isothermal calorimetry experiments. The isothermal heat of hydration curve was measured for a 24-h period directly following mixing; the immediate peak when the water contacted the cement-metakaolin-ZnO powder was not examined in this study.

An average hydration curve and standard error, taken from triplicate tests from three separate batches, was determined for each sample tested. From these hydration curves the end of the induction period (i.e. the start time of the acceleratory period) was determined as the time of last observed thermal minimum taken from the rate of heat evolution vs. time curve. Bentz et al. [36] demonstrated hydration curves using isothermal calorimetry were not a reliable indication of setting time (a physical process) for cement pastes. Therefore, only the chemical retardation (h), referring to the difference in the length of the induction period of ZnO containing pastes relative to non-ZnO containing pastes, was determined using Eq. (3).

$$R_s = T_z - T_c \tag{3}$$

where R_s (h) is the chemical retardation or the difference between induction periods for ZnO-containing samples relative to non-ZnO containing samples, T_z (h) is the end of the induction period for samples containing ZnO and T_c (h) is the end of the induction period for the control (non-ZnO containing sample).

Using the average hydration curves a linear trendline was fit between the minimum and maximum peak values of the average hydration curve to determine the ascending slope of the rate of heat evolution (J/g h^2). For samples with long induction periods (namely cement-metakaolin mixtures with 1.0% ZnO calcined at 500 °C and 550 °C and cement-metakaolin mixtures with 1.0% ZnO added post calcination), a minimum value was taken to be 2 J/h/g for more consistent curve fitting. All linear trendlines fitted to calculate the ascending slope had an R^2 value greater than or equal to 0.97.

XRD was used to determine the crystalline hydration products from zinc-containing metakaolin-cement pastes. Cu Kα radiation was used over a scan range of 5–60° 2θ in increments of 0.02° 2θ using a Siemens Diffraktometer. Paste mixtures contained a water-to-cementitious material ratio of 0.4 by mass and 0 wt% or 15 wt% metakaolin substitute for cement. The metakaolins used contained 0 wt% or 1 wt% ZnO additions and were fired at the prescribed calcination temperatures (500 °C, 550 °C, 600 °C, 650 °C). Following 21 h of hydration, samples were ground smaller than 45 μm and subjected to an ethanol flushing-vacuum filtration technique to stop hydration prior to XRD analysis. The hydration time frame of 21 h was selected to enable all paste mixtures to exceed the time required to reach the maximum peak of the heat of hydration.

2.5. Pozzolanic reactivity

Following French standard NF P18-513, the Chapelle test [37], the pozzolanic reactivity of metakaolin samples calcined at 500 °C and 650 °C, with and without 1 wt% ZnO additions, was conducted. For this test 2 g of calcium oxide (Fisher Scientific, 97 + %) was mixed with 1 g of sample in 250 ml of deionized water and placed onto a stirring–heating pad for 16 h at 80 °C. At the end of 16 h, the mixture was allowed to cool to 23 °C and 60 g of sucrose (Fisher Scientific) with 250 ml of deionized water was added. The resulting solution was filtered using 1 μm diameter filter paper. Six drops of a 0.1% phenolphthalein, 50% ethanol solution was added to 25 ml of the filtered solution, followed by the titration of 0.1 N hydrochloric acid solution. The titration reactions are shown in Eqs. (4) and (5). The results from this titration were used to determine the amount of calcium hydroxide (mg) fixed by the metakaolin or metakaolin-ZnO system. Duplicate tests with metakaolin from different batches were conducted to ensure repeatability.

$$\mathrm{CaO + 2HCl \rightarrow CaCl_2 + H_2O} \tag{4}$$

$$\mathrm{Ca(OH)_2 + 2HCl \rightarrow CaCl_2 + H_2O} \tag{5}$$

Pozzolanic reactivity was also monitored by comparing crystalline hydration products, namely the peak values of the calcium hydroxide and C_3S at pastes ages of 7 day and 28 days. Pastes were made with a water-to-cementitious material ratio of 0.4 by mass and 0 wt% or 15 wt% metakaolin substitute for cement. As with the Chapelle test, metakaolin samples calcined at 500 °C and 650 °C, with and without 1 wt% ZnO additions were used as the SCM portion of the paste. Cu Kα radiation was used over a scan range of 5–60° 2θ in increments of 0.02° 2θ using a Siemens Diffraktometer.

2.6. Compressive strength

The compressive strengths of 50 mm mortar cube specimens were tested per ASTM C109 [27]. Compressive strength testing was repeated three times for each mixture type using independently-calcined metakaolins each time. Mortars consisted of Type I Portland cement (Table 1) with 0 wt% or 15 wt% metakaolin substitute and Ottawa silica sand (Table 2). The metakaolins tested included 0 wt% or 1.0 wt% ZnO addition and were calcined at each prescribed calcination temperature (500 °C, 550 °C, 600 °C, 650 °C). Mixing procedures for mortars followed ASTM C305 specifications with nine cubes cast per batch [38]. Compressive strength specimens were demolded after 24 h and placed in a lime-water bath at 23 °C until testing. Three cubes were tested from a single batch at each age of 3, 7, and 28 days. Therefore, for a given age and mixture-type, nine specimens were tested, three cubes from three independent batches.

3. Results and discussion

3.1. Dehydroxylation

DSC and TGA were used to determine the effects of ZnO additions on the degree of dehydroxylation of the kaolinite heated to different temperatures. The results of DSC and TGA testing showed common kaolinite phase change characteristics, namely (i) mass loss due to evaporative water around 105 °C, (ii) an endothermic peak associated with the elimination of structural hydroxyl groups during dehydroxylation and associated thermogravimetric mass loss at a temperature range of 500–800 °C, and (iii) an exothermic peak associated with structural re-organization between 940 and

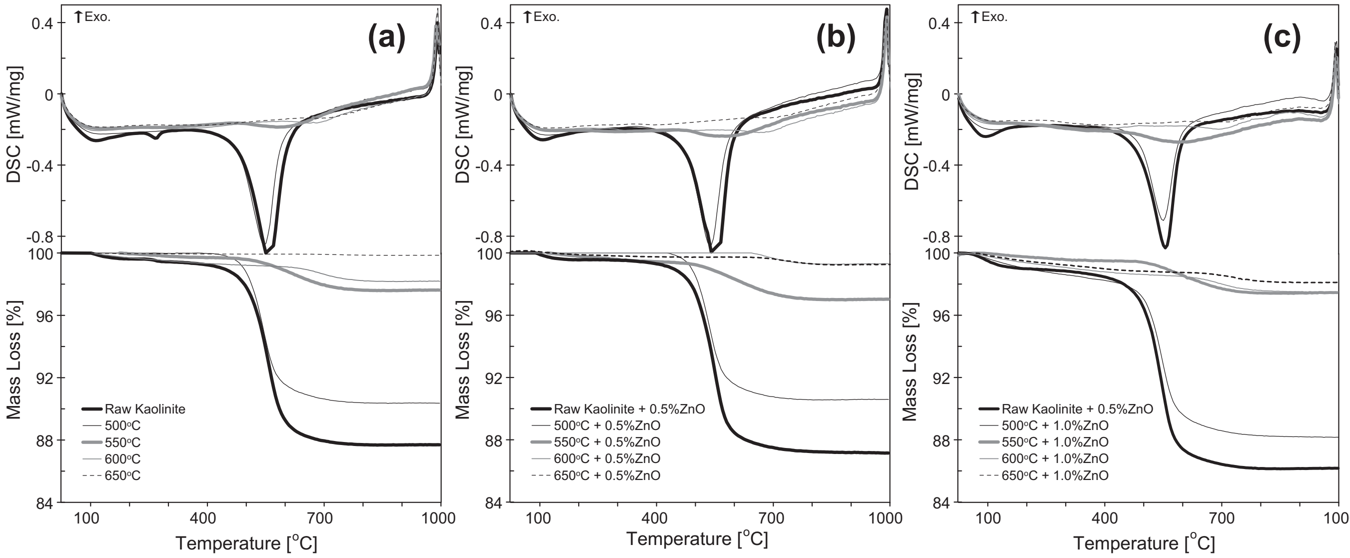

Fig. 2. DSC–TGA analysis of kaolinite (a) with no added flux and, (b) with 0.5 wt% addition of ZnO and (c) with 1.0 wt% addition of ZnO at (1) ambient, (2) 500 °C, (3) 550 °C, (4) 600 °C and (5) 650 °C, calcination temperatures.

1000 °C coupled with no mass loss (Fig. 2a–c). As the calcination temperature increased, the loss of hydroxyl groups increased, the area of the endothermic peak decreased, and the apex of the endothermic curve slightly shifted toward a higher calcination temperature (Fig. 2a–c).

The results show that thermal activation of kaolinite at 500 °C for 1 h achieved a low percentage of dehydroxylation (~12%). However, an increase of 50 °C in calcination temperature achieved ~75% dehydroxylation for both kaolinite samples with and without ZnO additions. At 650 °C, greater than 85% dehydroxylation was achieved (Table 3). Duplicate batches for two-thirds of the samples was conducted and yielded an approximate error for the degree of dehydroxylation of ±6.5% (Table 3). Therefore, there were no significant differences in degree of dehydroxylation between ZnO and non-ZnO containing samples. It can be concluded that, within the testing error, ZnO addition does not change the percent dehydroxylation at a specific calcination temperature.

The kaolinite crystalline composition was quantified using X-ray diffraction (XRD) analysis, to determine the effect of ZnO and calcination temperature on the structure of the calcined kaolinite. Increased calcination temperature decreased the percentage of crystalline kaolinite, shown by the emergence of an amorphous hump between 20 and 30° (2θ) at 550 °C and the disappearance of characteristic kaolinite peaks (hkl 001 and 002) at 600 °C (Fig. 3a and b). The kaolinite peak intensity for hkl 001 and 002 indicates the quantity of non-dehydroxylated kaolinite. There were slight variations in peak intensities between samples with and without ZnO additions. However, duplicate scans demonstrated that the variation was within sample error and not significant. Characteristic crystalline ZnO peaks were identified for samples with 1 wt% ZnO additions. The characteristic hkl 100 and 101 was found at 31.77° (2θ) 36.25° (2θ) for all calcination temperatures, with the intensity for these peaks most noticeable at the calcination temperature of 650 °C (Fig. 3b). The results were in

Table 3
DSC results for samples with 0.0 wt%, 0.5 wt%, 1.0 wt% ZnO flux additions, at ambient and calcination temperatures of 500–650 °C at intervals of 50 °C. Calculations were made per Eq. (1).

Sample	Endothermic peak (W/g)	Area of endothermic peak (J/g)	Degree of dehydroxylation (J/g)
Not calcined			
No ZnO	−0.92	−356	Base line
0.5 wt%ZnO	−0.96	−357	Base line
1.0 wt%ZnO	−0.82	−291	Base line
Calcination temperature 500 °C			
No ZnO	−0.85	−315	11.52
0.5 wt%ZnO	−0.85	−313	12.32
1.0 wt%ZnO	−0.71	−250	14.09
Calcination temperature 550 °C			
No ZnO	−0.19	−84.11	76.37
0.5 wt%ZnO	−0.24	−93.96	73.68
1.0 wt%ZnO	−0.27	−97.94	66.34
Calcination temperature 600 °C			
No ZnO	−0.15	−43.14	87.88
0.5 wt%ZnO	−0.22	−62.33	82.54
1.0 wt%ZnO	−0.23	−53.25	81.70
Calcination temperature 650 °C			
No ZnO	−0.14	−29.79	91.63
0.5 wt%ZnO	−0.13	−32.47	90.90
1.0 wt%ZnO	−0.15	−39.54	86.41

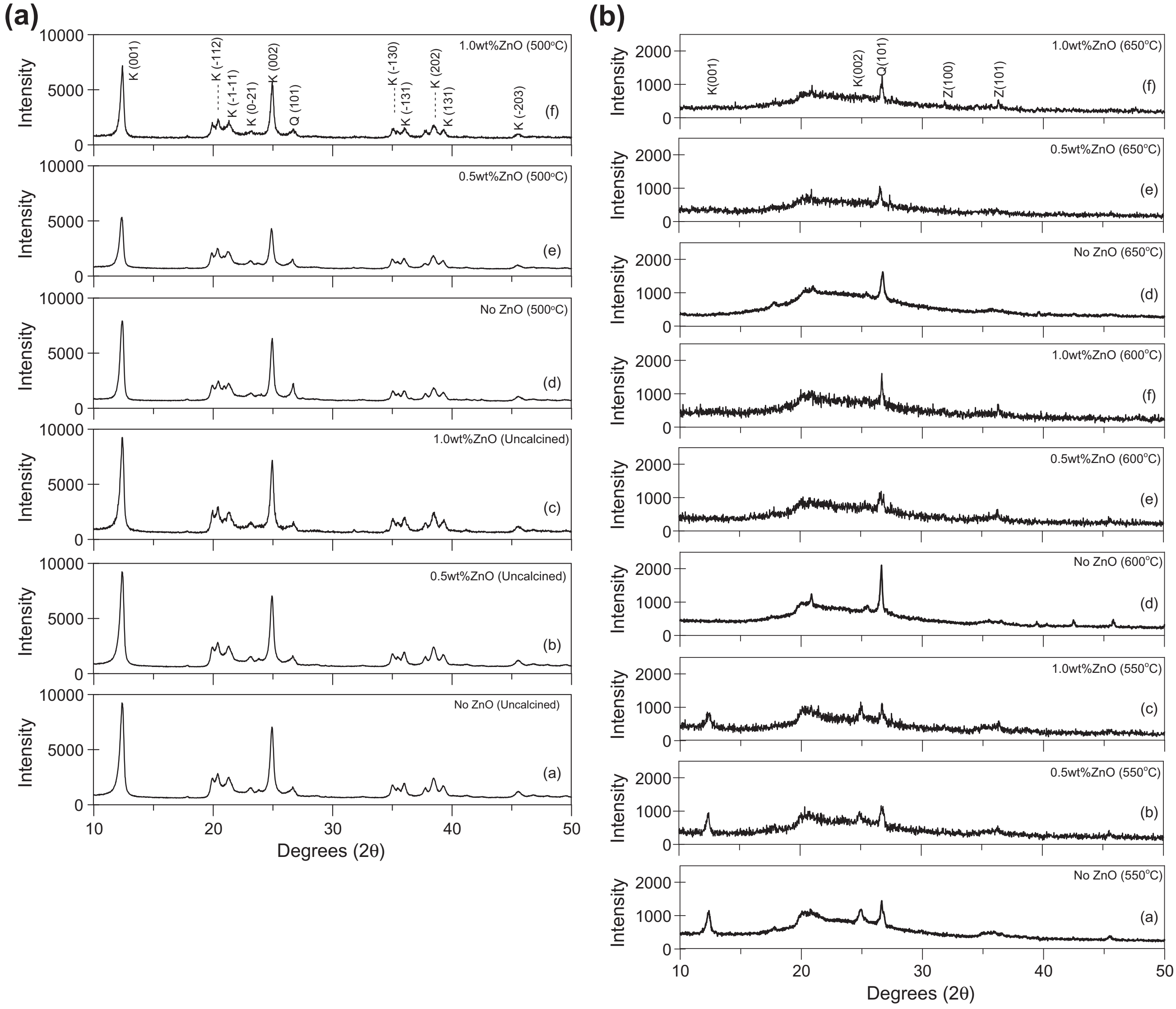

Fig. 3. XRD analysis of kaolinite with 0 wt%, 0.5 wt% and 1.0 wt% ZnO additions to kaolinite (a) uncalcined and calcined at a temperature of 500 °C and (b) calcined at temperatures of 550 °C, 600 °C and 650 °C. Where 'Q' represents quartz (SiO_2), 'Z' represents zinc oxide (ZnO) and 'K' represents kaolinite ($Al_2Si_2O_5(OH)_4$).

agreement with the DSC data that ZnO has no effect on the dehydroxylation of metakaolin.

Solid-state ^{27}Al and ^{29}Si MAS NMR were used to examine the effect of ZnO addition on the structure of metakaolin. The results from solid-state ^{27}Al and ^{29}Si MAS NMR are shown in Figs. 4 and 5, respectively. Published ^{27}Al spectra of uncalcined kaolinite contain only one signal centered at −3.0 ppm assigned to 6-coordinated Al (^{VI}Al) [39]. A chemical shift and the emergence of two weak signals indicate changes in the aluminum coordination resulting from dehydroxylation. The ^{27}Al spectrum of the metakaolin in Fig. 4 (calcination temperature 650 °C) contains a primary signal centered at −5.0 ppm, assigned to the 6-coordinated Al (^{IV}Al), with the chemical shift confirming dehydroxylation. Two additional weak signals near −21 and −50 ppm (Fig. 4) correspond to 5-coordinated Al (^{V}Al) and 4-coordinated Al (^{IV}Al), respectively.

Published ^{29}Si spectra of uncalcined kaolinite contain a signal centered around −91.6 ppm assigned to a Q^3 Si environment [39]. The ^{29}Si spectra in Fig. 5 shows a sharp peak at −94 ppm indicating that the layered Q^3 environment is still present, but is shifting toward the −99 ppm to −104 ppm realm, which is characteristic of metakaolin [39–41] (Fig. 5). The ^{29}Si spectra of samples containing no ZnO have a higher intensity peak at −94 ppm indicating a higher quantity of non-dehydroxylated kaolinite, relative to 1 wt% ZnO containing samples. However, given that the DSC/TGA and XRD results showed variation in the degree of dehydroxylation between ZnO and non-ZnO containing samples, but differences were within the relative error, it is likely that the differences in the NMR results are also due to variations between samples and not due to ZnO. Further testing would be needed to verify a change in metakaolin structure due to ZnO; for the purposes of this study it is concluded, based on the experimental results shown, that ZnO does not appreciably change the structure of metakaolin.

3.2. Hydration

Isothermal calorimetry was used to test the effects of metakaolin and ZnO on the hydration of Portland cement; results are shown in Fig. 6a–f. Each sample type was tested three times; each curve in Fig. 6 represents the average of the three tests. Results are shown for cement pastes with 85 wt% cement and 15 wt%

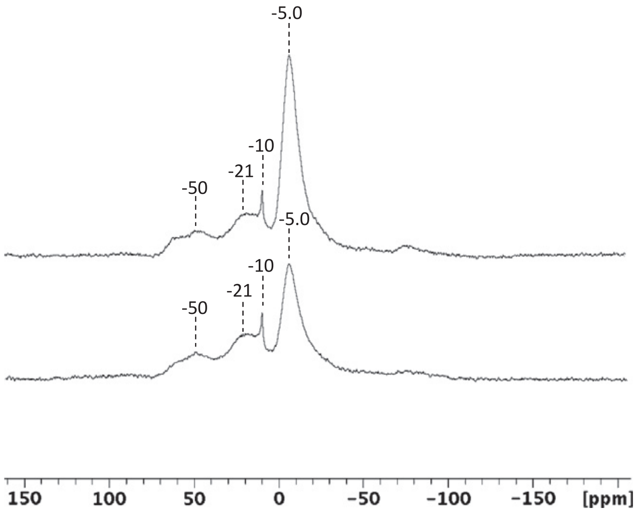

Fig. 4. The ^{27}Al{^{1}H} MAS NMR spectra at a spinning rate of 7 kHz. From top to bottom: metakaolin and metakaolin calcined with 1 wt% ZnO, (650 °C).

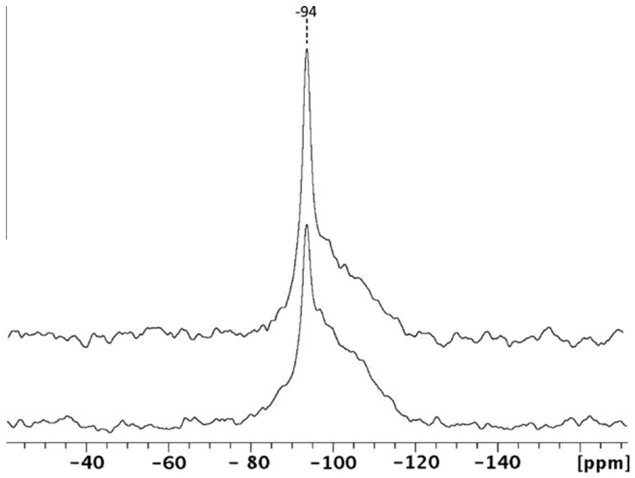

Fig. 5. The ^{29}Si{^{1}H} CP MAS NMR spectra at a spinning rate of 7 kHz. From top to bottom: metakaolin and metakaolin calcined with 1 wt% ZnO, (650 °C).

metakaolin containing 0 wt%, 0.1 wt%, 0.5 wt% or 1.0 wt% ZnO additions calcined with the kaolinite at four calcination temperatures (500 °C, 550 °C, 600 °C, and 650 °C). These results are compared to 100% cement pastes and 100% cement pastes with ZnO additions. The data deduced from Fig. 6c–f are shown in Table 4 and include the length of the induction period (h), chemical retardation (h), average maximum peak (J/g/h), the amount of time to reach this peak (h), the slope of acceleratory period (J/g h^{2}) and the cumulative heat evolved (J/g). The errors shown in Table 4 represent the standard deviations from triplicate tests.

Fig. 6a shows 100 wt% cement, 100 wt% cement with 0.15 wt% ZnO, and 85% cement 15 wt% metakaolin, with 1.0 wt% ZnO addition added pre- and post-calcination for metakaolinscalcined at 650 °C (note that 1.0 wt% ZnO by weight of metakaolin is equivalent to 0.15% of ZnO by weight of cementitious materials). The data presented in Fig. 6a are only for using Cement B; the rest of the results shown are for Cement A. Fig. 6a shows that cement paste with 0.15 wt% ZnO addition has a chemical retardation of approximately 27 h followed by an increase in the apex of the hydration curve of 33% compared with a neat cement system. The retardation in the cement-ZnO system is in agreement with the literature [15,16]. In fact, the behavior of the ZnO in the cement paste is more indicative of a 'delayed accelerator' than a pure retarder, such that once the inhibition period has ended hydration proceeds at a faster rate than when no retarder has been added [42–45].

Fig. 6a also shows a reduction in the apex of the heat of hydration by approximately 15% for the 85 wt% cement 15 wt% metakaolin system, demonstrating that metakaolin is relatively inert during early hydration at 3 h to 24 h, in agreement with the literature [7]. The 15% reduction in heat of the metakolin-cement system with no zinc is eliminated with the addition of 1 wt% ZnO, showing that the lost reactivity in early hydration can be overcome by the addition of ZnO. In addition, any chemical retardation exhibited by the pure cement-ZnO system is eliminated with the addition of the metkaolin, showing that the metakaolin can act as a buffer, reducing chemical retardation caused by ZnO-cement interactions.

Furthermore, no differences in the heat of hydration could be shown when ZnO was added to kaolinite before calcination or after calcination (Fig. 6a). These results are in agreement with the DSC/TGA, XRD and NMR results which essentially demonstrated no structural differences between metakaolins calcined with ZnO compared to pure metakaolin. The fact that hydration is not sensitive to co-calcination allows for zinc-containing compounds to be simply added to a metakaolin-cement blend.

Overall the results in Fig. 6a demonstrate two critical objectives in this study: (1) ZnO has the potential of offsetting the reduction in early hydration due to an inert or slowly reacting SCM and (2) metakaolin enables the use of ZnO in concrete without retardation, opening the door to a variety of ZnO compounds, such as electric arc furnace dust to be successfully used in concrete.

Fig. 6b shows the hydration of metakaolin-cement paste with no ZnO, calcined at the four different calcination temperatures (500 °C, 550 °C, 600 °C, and 650 °C). From Fig. 6b the degree of dehydroxylation does not affect the early reactivity of the metakaolin-cement blend confirming that the metakaolin is inert during early hydration (first 24 h).

An investigation was conducted examining the influence of two variables: (1) the percentage of ZnO added to the kaolinite prior to calcination and (2) the influence of kaolinite dehydroxylation on the metakaolin-cement-ZnO system. Fig. 6c–f shows an increase in the apex of the heat of hydration curve for metakaolin with increasing wt% ZnO. For example, the hydration peak height for non-ZnO samples ranged from 16 ± 0.5 J/h/g to 17 ± 0.4 J/h/g depending on the calcination temperature. 1.0 wt% ZnO addition increased the average hydration peak height by 26–32% (ranging from 21.1 ± 0.9 J/h/g to 23.5 ± 0.5 J/h/g depending on calcination temperature). Fig. 7a plots the maximum peak height as a function of the wt% ZnO addition for each calcination temperature, with the error line representing the standard deviation from triplicate testing (~5%). A linear relationship, independent of calcination temperature, is shown in Fig. 7a showing a clear correlation between increased wt% ZnO additions and increased peak height.

Coupled with the increase in the peak of the hydration curve with ZnO addition was an increase in the chemical retardation for metakaolins with decreasing dehydroxylation content. Fig. 7b shows the average chemical retardation (Eq. (3)) as a function of the wt% ZnO addition for each calcination temperature. Negative results signify that samples containing ZnO additions had shorter induction periods than control samples (i.e. samples with no ZnO additions). Samples containing 1.0 wt% ZnO and having the largest degree of dehydroxylated kaolinite exhibited the least chemical retardation (Table 3). Samples with long induction periods also had a delay in the time to reach the hydration peak and a lower cumulative heat at 24 h (Table 4). Overall, the chemical retardation of the metakaolin-cement paste with 1 wt% ZnO could be reduced only by using the highest calcination temperature of 650 °C.

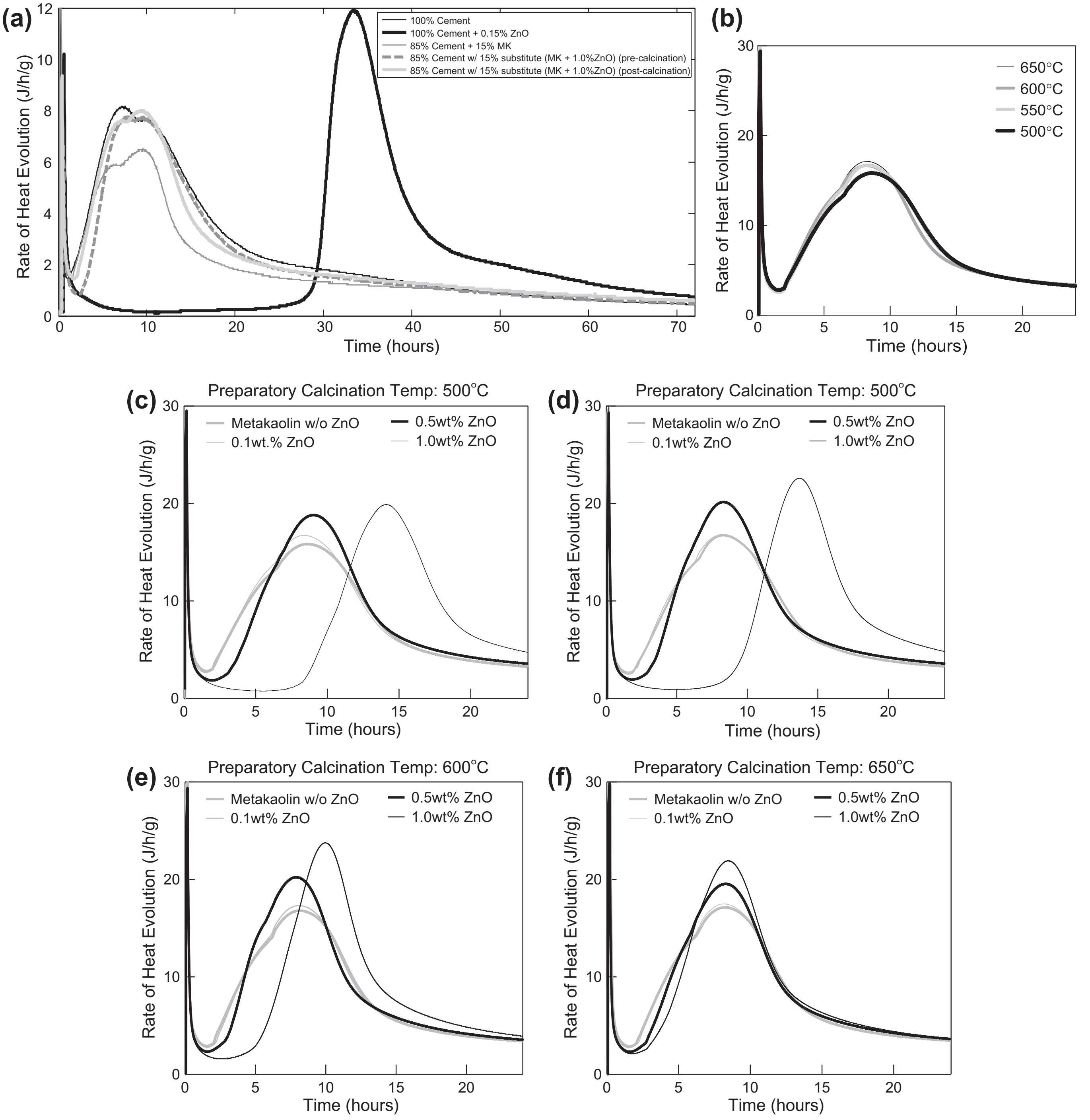

Fig. 6. The rate of heat evolution (J/h/g) vs. time (h) for cement pastes containing (a) 100 wt% cement, 100 wt% cement + 0.15 wt% ZnO, cement with a substitute of 15 wt% metakaolin with 1.0 wt% ZnO addition added pre and post calcination; (b) cement with a substitute of 15 wt% metakaolin for calcinations temperatures of 500 °C, 550 °C, 600 °C, 650 °C; cement pastes containing 15 wt% metakaolin, with 0 to 1.0 wt% ZnO flux addition, for calcinations temperatures of (c) 500 °C, (d) 550 °C, (e) 600 °C and (f) 650 °C. *Note*: 6(a) used cement B and the remaining plots used cement A.

Fig. 7c shows the ascending slope (J/g h^2) determined from the average heat of hydration curve established from three calorimetry tests per sample as a function of the wt% ZnO additions at 500 °C, 550 °C, 600 °C and 650 °C calcination temperatures. The ascending slope is an indication of the rate of reaction during this time period. A linear relationship was determined showing an increase in the slope as the wt% ZnO additions increase ($R^2 = 0.85$).

The XRD scans of paste mixtures dried and crushed at 21 h containing 15 wt% metakaolin fired at the prescribed calcination temperatures (500 °C, 550 °C, 600 °C, 650 °C) with 1 wt% ZnO additions are shown in Fig. 8 and summarized in Table 6. The XRD results revealed that no zinc crystalline phases formed in the pastes. The crystalline phase calcium zincate ($CaZn_2(OH)_6{\cdot}2H_2O$) was reported in the literature to reduce the pozzolanic reaction between $Ca(OH)_2$ and fly ash in systems containing no Portland cement [25]; this phase was not detected in the present study. The principal crystalline cement phases and hydration products C_3S,C_2S, CH, and ettringite ($C_6A\hat{S}_3H_{32}$) were identified in the hydrated pastes. The relative degree of hydration of the cement can be roughly determined by analyzing the peak intensity of the C_3S. Pastes

Table 4
Hydration parameters from isothermal calorimetry for samples containing no flux and additions of 0.1 wt%, 0.5 wt% and 1.0 wt% ZnO flux for the four calcination temperatures (500 °C, 550 °C, 600 °C, 650 °C). The cumulative heat is taken at 24 h following mixing.

Sample	Induction period (h)	Chemical retardation (h)	Maximum peak (J/h/g)	Time to maximum peak (h)	Ascending slope (J/g/h^2) (10^{-3})	Cumulative heat (J/g)
Calcination temperature 500 °C						
No ZnO	1.7 ± 0.04	Baseline	15.95 ± 0.53	8.45 ± 0.59	5.6	195.98 ± 0.99
0.1 wt%ZnO	1.7 ± 0.07	−0.01	16.77 ± 0.40	7.89 ± 0.16	6.3	197.65 ± 0.82
0.5 wt%ZnO	2.3 ± 0.51	0.59	18.94 ± 0.88	8.81 ± 0.53	8	200.46 ± 3.79
1.0 wt%ZnO	7.6 ± 1.59	5.89	21.07 ± 0.92	15.04 ± 2.42	11.1	182.20 ± 9.18
Calcination temperature 550 °C						
No ZnO	1.7 ± 0.04	Baseline	16.72 ± 0.09	8.06 ± 0.19	6.4	198.63 ± 1.15
0.1 wt%ZnO	1.7 ± 0.06	0	16.84 ± 0.25	8.09 ± 0.03	6.4	197.73 ± 1.34
0.5 wt%ZnO	2.0 ± 0.23	0.37	20.66 ± 0.40	8.16 ± 0.50	9.6	206.05 ± 2.26
1.0 wt%ZnO	6.1 ± 0.19	4.36	23.00 ± 0.36	13.64 ± 0.53	13.2	187.07 ± 3.67
Calcination temperature 600 °C						
No ZnO	1.7 ± 0.01	Baseline	16.79 ± 0.18	8.00 ± 0.06	6.5	198.23 ± 1.17
0.1 wt%ZnO	1.7 ± 0.06	0	17.32 ± 0.44	7.91 ± 0.04	7.1	196.85 ± 2.92
0.5 wt%ZnO	1.8 ± 0.19	0.08	20.27 ± 0.43	7.77 ± 0.34	9.7	205.77 ± 3.14
1.0 wt%ZnO	4.6 ± 1.35	2.91	23.52 ± 0.46	12.11 ± 2.18	13.5	195.73 ± 11.24
Calcination temperature 650 °C						
No ZnO	1.7 ± 0.04	Baseline	17.14 ± 0.40	8.06 ± 0.25	6.6	199.99 ± 1.39
0.1 wt%ZnO	1.65 ± 0.04	−0.06	17.48 ± 0.39	8.02 ± 0.16	6.9	200.18 ± 0.44
0.5 wt%ZnO	1.8 ± 0.35	0.11	19.94 ± 0.53	8.06 ± 0.74	7.3	205.52 ± 0.44
1.0 wt%ZnO	1.8 ± 0.31	0.17	22.57 ± 0.55	8.93 ± 0.82	10	210.79 ± 3.91

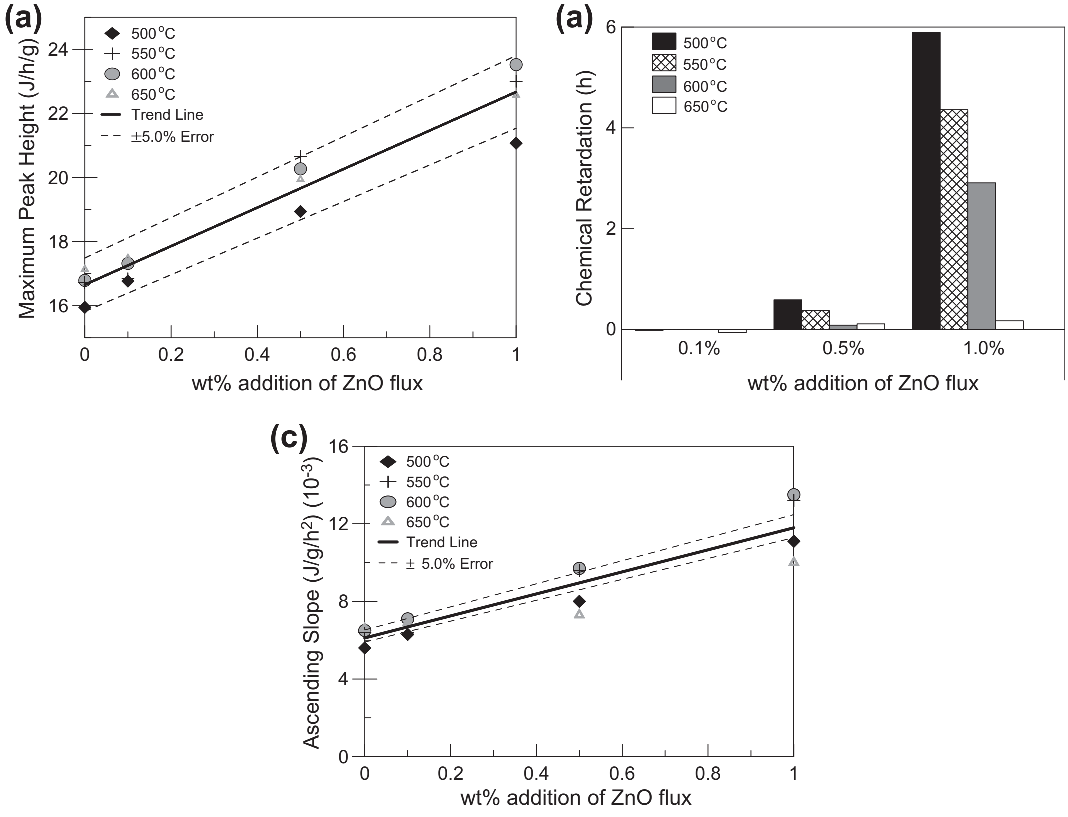

Fig. 7. (a) The maximum peak height (J/h/g) ± 5.0% error, (b) the chemical retardation to reach initial set (h) and, (c) the average ascending slope (J/g h^2) ± 5.0% error, all as a function of the wt% ZnO additions at calcination temperatures of 500 °C, 550 °C, 600 °C and 650 °C.

containing metakaolin calcined at 500 °C and 550 °C showed greater C_3S peak intensity (*hkl* 021, 024 and 009) than samples calcined at 600 °C and 650 °C (Fig. 8, Table 6). The XRD data are in agreement with calorimetry results, which showed samples with increased calcination temperatures reach the peak of hydration at a faster rate than samples with lower calcination temperatures (Fig. 6c–f), resulting in the more rapid consumption of C_3S to form C–S–H and crystalline CH hydration products. Additionally, the results confirm the disappearance of the primary and secondary kaolinite peaks (*hkl* spacing of 001 and 002) for kaolinite fired at 600 °C, in agreement with Fig. 3b.

3.3. Pozzolanic reactivity

While early-age isothermal calorimetry demonstrates the effects of additives on the early hydration rate of cement, it provides

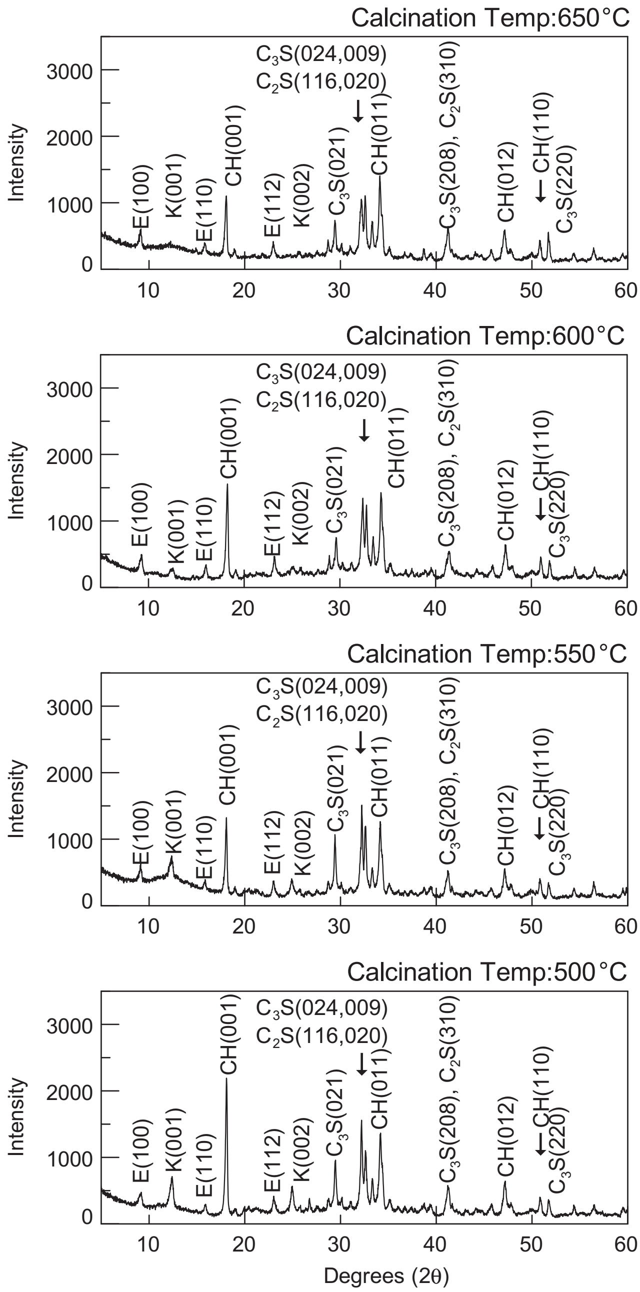

Fig. 8. XRD scans of paste mixtures dried and crushed at 21 h containing 15 wt% metakaolin substitute, fired at the prescribed calcination temperatures (500 °C, 550 °C, 600 °C, 650 °C) with 1 wt% ZnO additions. 'E' represents ettringite ($C_6A\hat{S}_3H_{32}$) and 'K' represents kaolinite ($A_2S_2O_5(OH)_4$).

little information on the pozzolanic reaction, which occurs later. The Chapelle test was therefore used to examine pozzolanic reactivity of the materials. No differences were shown in the results from the Chapelle test for samples with and without 1 wt% ZnO additions (Table 5), indicating that the addition of ZnO to kaolinite prior to calcination does not change the pozzolanic reactivity of the metakaolin. Samples calcined at 650 °C fixed 1758 ± 22 mg of calcium hydroxide, slightly less than metakaolin samples with 1 wt% ZnO, which fixed 1825 ± 10 mg, but within error. Samples calcined at 500 °C had a reduction in the amount of fixed calcium hydroxide by more than 50%, exhibiting less pozzolanic reactivity compared to metakaolins calcined at 650 °C (Table 5). The results from the Chapelle test in this study are within the range of Kakali et al. [46]. The amount of fixed calcium hydroxide has been shown to vary due to the crystallinity of the original kaolinite, where less ordered kaolinites exhibit a higher reactivity [46].

As stated earlier, methods of increasing the reactivity of SCMs to enable the use of less reactive material can be effective by either compensating for the dilution effect due to the 15 wt% substitute of SCM which becomes reactive at later stages of hydration or by increasing pozzolanic reactivity. According to the Chapelle test results, it appears that ZnO additions to metakaolin-cement blends achieve the former, but not the latter.

To further investigate the pozzolanic reactivity, XRD scans of pastes were conducted at the ages of 7 and 28 days. These data are shown in Fig. 9a–d and are summarized in Table 6 along with the 21 h data discussed earlier. Each calcium hydroxide peak (hkl 001, 011, 012) was respectively the same across all 21 h scans, regardless of the calcination temperature of the metakaolin. Therefore, the formation of calcium hydroxide at this time is due to the hydraulic reactions. A reduction in CH peak height between 21 h and 7 day scans is due to the pozzolanic reactions from the metakaolin. Pastes containing metakaolincalcined at 500 °C showed greater C_3S and C_2S peak greater CH intensities and greater kaolinite peak intensities, than samples calcined at 650 °C, at both 7 and 28 days (Fig. 9a–d, Table 6), indicating a lower degree of cement reaction and lower pozzolanicity. These results are in agreement with finding from the DSC/TGA and Chapelle tests, where the higher calcination temperature resulted in a larger degree of dehydroxylated kaolinite and was therefore more pozzolanically reactive. There is some variation in the primary calcium hydroxide peak (hkl 001) height between samples containing ZnO and non-ZnO samples (Table 6). However, the differences are minimal and within error. Overall, the XRD scans demonstrated differences in the pozzolanic reactivity are influenced more by calcination temperature than ZnO addition.

3.4. Compressive strength

Fig. 10a–c shows the mortar cube compressive strengths (MPa) for (a) 3-day, (b) 7-day and (c) 28-day specimens for mortars with neat cement (control), 15 wt% metakaolin (no ZnO), and metakaolin with 1 wt% ZnO calcined at each temperature (500 °C, 550 °C, 600 °C, 650 °C). The average compressive strength was taken from

Table 5
Results from the Chapelle test.

Sample	Calcination temperature (°C)	$\frac{mg\ (Ca(OH)_2)}{g\ (sample)}$	Standard deviation (mg/g)
Metakaolin	500	731.64	6.47
Metakaolin w/l wt% ZnO	500	877.22	6.47
Metakaolin	650	1761.90	17.11
Metakaolin w/l wt% ZnO	650	1825.36	5.60

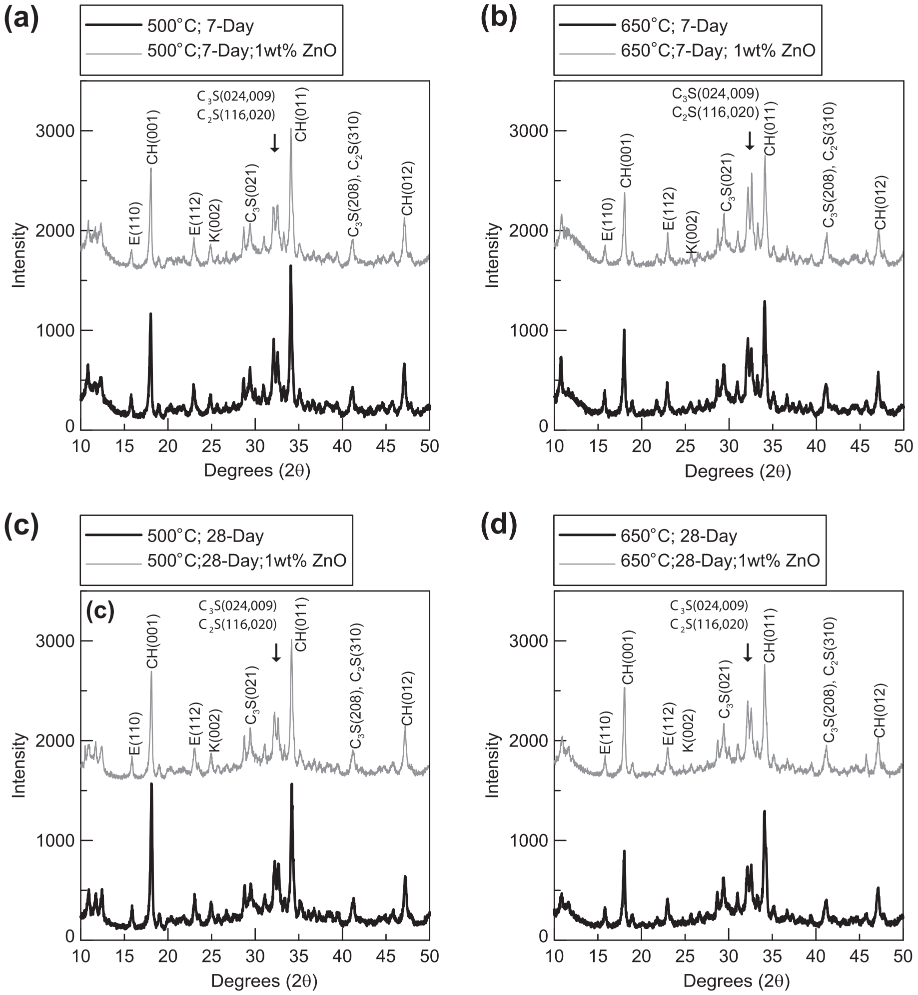

Fig. 9. XRD scans of paste mixtures dried and crushed at 7 and 28 days containing 15 wt% metakaolin substitute, fired at the prescribed calcination temperatures (500 °C and 650 °C) with 1 wt% ZnO additions. 'E' represents ettringite ($C_6A\hat{S}_3H_{32}$) and 'K' represents kaolinite ($A_2S_2O_5(OH)_4$), CH represents calcium hydroxide ($Ca(OH)_2$).

three replicate batches with three cubes tested at each age for each sample type.

The 3-day compressive strength results reveal that substitution of 15 wt% metakaolin for cement lowered the early compressive strength when the metakaolin was incompletely calcined (500 °C with and without ZnO and 550 °C without ZnO), but had no significant effect on 3-day strength at high calcination temperatures (Fig. 10a). At 7 days, the average compressive strength of mortars containing 1 wt% ZnO-kaolinite calcined at 650 °C was stronger than all other samples (Fig. 10b). Mortars with metakaolin and 1 wt% zinc additions maintained comparable strength relative to metakaolin mortars without ZnO.

The 28-day compressive strength results (Fig. 10c) followed the same trends as the 7-day results. Strength was significantly higher for metakaolin with 1 wt% ZnO calcined at 650 °C compared to all other samples. Both ZnO and non-ZnO samples calcined at 650 °C achieved greater compressive strengths than the control (containing no metakaolin), which is expected given the pozzolanic reaction of the SCM. Metakaolins which were incompletely calcined lowered strength compared to the control.

It is surprising that the metkaolin calcined at 650 °C with 1 wt% ZnO had a higher compressive strength than the mortar containing a similar metakaolin without ZnO considering that the Chappelle test suggested no change in pozzolanic reactivity due to ZnO. This could be because the Chappelle test is a convenient, but imperfect method of measuring pozzolanic reactivity since it measures reac-

Table 6
The peak intensity taken from the XRD scans shown in Figs. 8 and 9.

Peak intensity (metakaolin calcined at 500 °C)						
		l wt% ZnO	No ZnO	l wt% ZnO	No ZnO	l wt% ZnO
	hkl	21 hr.	7 day	7 day	28 day	28 day
$Ca(OH)_2$	(001)	2041	1013	1226	1419	1049
$Ca(OH)_2$	(011)	1132	1353	1263	1336	1221
$Ca(OH)_2$	(012)	480	491	492	463	467
C_3S	(021)	731	410	501	337	337
C_3S	(024)	1281	601	475	563	463
C_2S	(016)					
C_3S	(009)	800	469	476	563	404
C_2S	(020)					
C_3S	(208)	451	255	236	233	229
C_2S	(310)					
Kaolinite	(001)	462	271	376	345	283
Kaolinite	(002)	374	177	224	211	198
Peak intensity (metakaolin calcined at 650 °C)						
$Ca(OH)_2$	(001)	890	829	628	731	858
$Ca(OH)_2$	(011)	1187	984	942	1005	947
$Ca(OH)_2$	(012)	441	404	348	353	344
C3S	(021)	502	427	460	356	383
C_3S	(024)	771	586	587	443	569
C_2S	(016)					
C_3S	(009)	797	484	518	444	487
C_2S	(020)					
C_3S	(208)	481	265	235	230	344
C_2S	(310)					
Kaolinite	(001)	na	na	na	na	na
Kaolinite	(002)	na	na	na	na	na

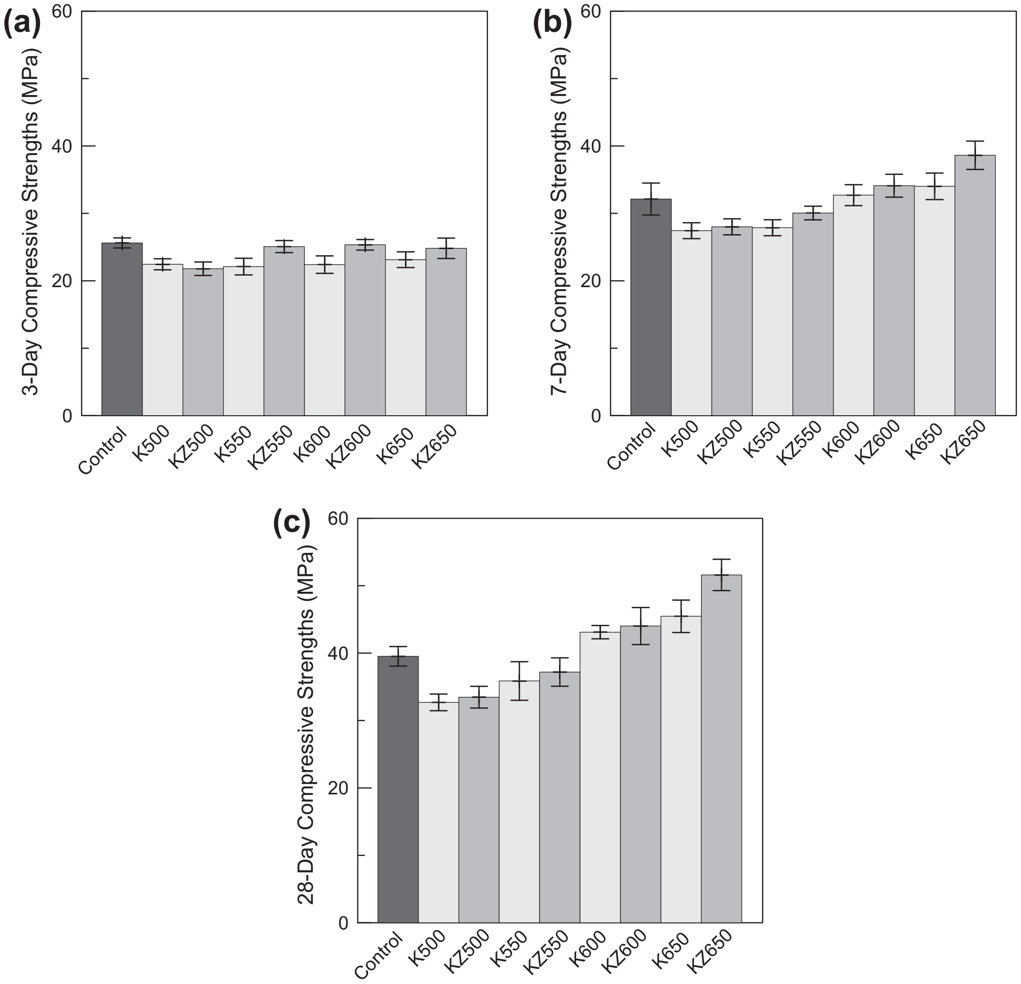

Fig. 10. Mortar cube compressive strengths (MPa) for (a) 3-days, (b) 7-days and (c) 28-days, consisting of cement-Ottawa sand mixtures with neat cement (control, shown in black), 15 wt% metakaolin-SCM from kaolinite calcined at each temperature (K500, K550, K600, K650, shown in light gray) and metakaolin-ZnO SCM from kaolinite and 1 wt% ZnO calcined together at each temperature (KZ500, KZ550, KZ600, KZ650, shown in dark gray).

tivity in an idealized lime solution rather than in a cementitious system [37]. It could also be that the presence of ZnO changes the microstructure in the cement-metakaolin system. Elucidation of the mechanism for this strength difference requires further investigation.

4. Conclusions

This study reported on the observed increased reactivity of metakaolin-cement systems with the addition of ZnO, demonstrating that an increase in early cement hydration compensated for any dilution effect caused by the SCM in the first 24 h. In the absence of metakaolin, ZnO behaved very similarly to sucrose, acting like a 'delayed accelerator' [42–45], with an extended induction period followed by an increased reaction rate during the acceleratory period of hydration. When combined with metakaolin, the retardation caused by ZnO was diminished (as a function of dehydroxylated content), however the reaction rate acceleration was preserved. The ability to utilize the increased rate of reaction may offset the low reactivity of poorly pozzolanic SCM, facilitating their use. Of particular interest in a future study is the use of impure calcined clays which are more accessible, inexpensive and require less manufacturing compared to pure metakaolin.

In this study it was shown that the degree of dehydroxylation and pozzolanicity of kaolinite were influenced by increasing the calcination temperatures, but not by ZnO additions. This was further supported by the fact additions of ZnO pre- or post-calcination resulted in the same rate of heat evolution. For both ZnO and non-ZnO containing samples calcined at 650 °C, greater than 85% dehydroxylated metakaolin was obtained; thus this temperature was determined to be the optimum calcination temperature for the materials and firing parameters used in this study. Paste and mortars containing metakaolin with increasing ZnO additions and increasing calcination temperature exhibited the following trends in heat flow during calorimetry testing: (i) an increase in the maximum peak height, (ii) a reduction in chemical retardation, (iii) a reduction in the time to reach the maximum peak, (iv) a steeper average ascending slope and, (v) an increase in the cumulative heat. In addition, the 7 and 28-day compressive strength results for mortars containing 1 wt% ZnO additions to kaolinite calcined at 650 °C showed slightly higher strengths relative to non-ZnO samples. For this study the optimal ZnO-metakaolin SCM was determined to contain 1 wt% ZnO calcined at 650 °C. This mixture showed minimal chemical retardation (10.2 min), an increase of ~26% in maximum heat flow during hydration, and 23% average improvement in compressive strength relative to Type I Portland cement mortar.

The findings from this study demonstrate it is possible to overcome the severe retardation associated with zinc compounds discussed in previous studies [15–18]. The use of metakaolin combined with ZnO virtually eliminates chemical retardation (for highly dehydroxylated metakaolin), allowing for a variety of ZnO-containing waste materials that could be used as concrete additives, such as electric arc furnace dust (EAFD).

Acknowledgments

This work was supported by the US Environmental Protection Agency STAR fellowship (Project No. FP-91717601-O) awarded to Sarah Taylor Lange and the National Science Foundation (Project No. CMMI 1030972, CMMI 1030939). Any opinions, findings, and conclusions expressed in this document are those of the authors and do not necessarily reflect those of the US Environmental Protection Agency and the National Science Foundation. The novel technique of outlined in this paper is part of a provisional patent (Serial No. 61/467114). The authors would like to acknowledge Dr. Vladimir Bakhmoutov and Steve Silber from the Texas A&M NMR facilities, Dr. Ben Shoulders of the University of Texas NMR facilities, Dr. Jorgen Skibsted, and Dr. Jeffrey Siegel for their help and advice.

References

[1] Coleman NJ, Page CL. Aspects of the pore solution chemistry of hydrated cement pastes containing metakaolin. Cem Concr Res 1997;27(1):147–54.
[2] Goncalves JP, Tavares LM, Toledo Filho RD, Fairbairn EMR. Performance evaluation of cement mortars modified with metakaolin or ground brick. Constr Build Mater 2009;23:1971–9.
[3] Siddique R, Klaus J. Influence of metakaolin on the properties of mortar and concrete: a review. Appl Clay Sci 2009;43:392–400.
[4] Sajidu SMI, Persson I, Masamba WRL, Henry EMT. Mechanisms of heavy metal sorption on alkaline clays from Tundulu in Malawi as determined by EXAFS. J Hazard Mater 2008;158:401–9.
[5] Sakizci M, Alver BE, Yörükoğullari E. Thermal behavior and immersion heats of selected clays from Turkey. J Therm Anal Calorim 2009;98:429–36.
[6] Samet B, Mnif T, Chaabouni M. Use of a kaolinite clay as a pozzolanic material for cements: formulation of blended cement. Cem Concr Compos 2007;29:741–9.
[7] Taylor HFW. Cement chemistry. 2nd ed. London: Thomas Telford Publishing; 1997.
[8] Badogiannis E, Papadakis VG, Chaniotakis E, Tsivilis S. Exploitation of poor Greek kaolins: strength development of metakaolin concrete and evaluation by means of *K*-value. Cem Concr Res 2004;34(6):1035–41.
[9] He C, Osbaeck B, Makovicky E. Pozzolanic reactions of six principal clay minerals: activation, reactivity assessments and technological effects. Cem Concr Res 1995;25(8):1691–702.
[10] Zhang MH, Malhotra VM. Characteristics of a thermally activated aluminosilicate, pozzolanic material and its use in concrete. Cem Concr Res 1995;25(8):1713–25.
[11] San Cristóbal AG, Castelló R, Luengo MAM, Vizcayno C. Acid activation of mechanically and thermally modified kaolins. Mater Res Bull 2009;44:2103–11.
[12] Lenarda M, Storaro L, Talon A, Moretti E, Riello P. Solid acid catalysts from clays: preparation of mesoporous catalysts by chemical activation of metakaolin under acid conditions. J Colloid Interf Sci 2007;311:537–43.
[13] Kuechler AH. Influence of Fe_2O_3 and TiO_2 on pure clays. J Am Ceram Soc 1926;9(1).
[14] Chatterji, Phatack, Dhariyal, Banerji. Pozzolanic activity of kaolin fire with admixtures of zinc oxide. J Sci Ind Res 1960;19B:453–4.
[15] Dyer T, Jones R, Garvin S. Exposure of Portland cement to multiple trace metal loadings. Mag Concr Res 2009;61(1):57–65.
[16] Al-Zaid RZ, Al-Sugair FH, Al-Negheimish AI. Investigation of potential uses of electric-arc furnace dust (EAFD) in concrete. Cem Concr Res 1997;27(2):267–78.
[17] Puertas F, García-Díaz I, Palacios M, Gazulla MF, Gómez MP, Orduña M. Clinkers and cements obtained from raw mix containing ceramic waste as a raw material. Characterization, hydration and leaching studies. Cem Concr Compos 2010;32:175–86.
[18] Berger S, Cau Dit Coumes C, Le Bescop P, Damidot D. Hydration of calcium sulfoaluminate cement by a $ZnCl_2$ solution: investigation at early age. Cem Concr Res 2009;39:1180–7.
[19] Farrah H, Pickering WF. The sorption of zinc species by clay minerals. J Chem 1976;29:1649–56.
[20] Farrah H, Pickering WF. pH effects in the adsorption of heavy metal ions by clays. Chem Geol 1979;25:317–26.
[21] Farrah H, Hatton D, Pickering WF. The affinity of metal ions for clay surfaces. Chem Geol 1980;28:55–68.
[22] Adebowale KO, Unuabonah IE, Olu-Owolabi BI. Adsorption of some heavy metal ions on sulfate- and phosphate-modified kaolin. Appl Clay Sci 2005;29:145–8.
[23] Unuabonah IE, Olu-Owolabi BI, Adebowale KO, Ofomaja AE. Adsorption of lead and cadmium ions from aqueous solutions by tripolyphosphate-impregnated kaolinite clay. Colloids Surf A: Physicochem Eng Asp 2007;282:202–11.
[24] Guerra DL, Airoldi C, de Sousa KS. Adsorption and Thermodynamic studies of Cu (II) and Zn(II) on organofunctionalized kaolinite. Appl Surf Sci 2008;254:5157–63.
[25] Amer MW, Fawwaz IK, Akl MA. Adsorption of lead, zinc and cadmium ions on polyphosphate-modified kaolinite clay. J Environ Chem Ecotoxicol 2010;2(1):001–8.
[26] American Society for Testing and Materials (ASTM) C150/C150M. Standard Specification for Portland Cement, Annual book of ASTM standards, West Conshohocken, PA; 2009.
[27] American Society for Testing and Materials (ASTM) C109/C109M. Standard Test Method for Compressive Strength of Cylindrical Concrete Specimens, Annual book of ASTM standards, West Conshohocken, PA; 2005.
[28] American Society for Testing and Materials (ASTM) C204. Standard Test Methods for Fineness of Hydraulic Cement by Air-Permeability Apparatus, Annual book of ASTM standards, West Conshohocken, PA; 2007.
[29] Mindess S, Young FJ, Darwin D. Concrete. 2nd ed. New Jersey: Pearson Education, Inc; 2003.
[30] Bich CH, Ambroise J, Pér J. Influence of degree of dehydroxylation on the pozzolanic activity of metakaolin. Appl Clay Sci 2009;44(3–4):194–200.
[31] American Society for Testing and Materials (ASTM) C1702-Method B. Standard Test Method for Measurement of Heat of Hydration of Hydraulic Cementitious Materials Using Isothermal Conduction Calorimetry. Annual book of ASTM standards, West Conshohocken, PA; 2009.
[32] Bentz DP. Transient plane source measurements of the thermal properties of hydrating cement pastes. Mater Struct 2007;40:1073–80.
[33] Xu Y, Chung DDL. Effect of sand addition on the specific heat and thermal conductivity of cement. Cem Concr Res 2000;30:59–61.
[34] Holman JP. Heat transfer. New York: McGraw-Hill; 1981.
[35] Robie RA, Hemingway BS. Heat capacities of kaolinite from 20 to 310 K, the entropy of kaolinite $Al_2SiO_2(OH)_4$. Clays Clay Miner 1991;39(4):362–8.
[36] Bentz DP, Peltz MA, Winpigler J. Early-age properties of cement-based materials. II: influence of water-to-cement ratio. J Mater Civ Eng 2009;21(9):512–7.
[37] Largent R. Estimation de l'activite pouzzolanique. Bull Liaison Lab Pont Chausees 1978;93:61.
[38] American Society for Testing and Materials (ASTM) C305/C305M, Standard Practice for Mechanical Mixing of Hydraulic Cement Pastes and Mortars of Plastic Consistency, Annual book of ASTM standards, West Conshohocken, PA; 2006.
[39] He HP, Guo JG, Zhu JX, Hu C. ^{29}Si and ^{27}Al MAS NMR study of the thermal transformations of kaolinite from north China. Clay Miner 2003;38:551–9.
[40] Rocha J, Klinowski J. ^{29} Si and^{27} Al magic-angle-spinning NMR studies of the thermal transformation of kaolinite. Phys Chem Miner 1990;17:179–86.
[41] Massiot D, Dion P, Alcover JF, Bergay F. ^{27} Al and^{29} Si MAS NMR study of kaolinite thermal decomposition by controlled rate thermal analysis. J Am Ceram Soc 1995;78:2940–4.
[42] Juenger MCG, Jennings HM. New insights into the effects of sugar on the hydration and microstructure of cement pastes. Cem Concr Res 2002;32(3):393–9.
[43] Peterson VK, Juenger MCG. Hydration of tricalcium silicate: effects of $CaCl_2$ and sucrose on reaction kinetics and product formation. Chem Mater 2006;18(24):5798–804.
[44] Young JF, Berger RL, Lawrence Jr FV. Hydration of tricalcium silicate pastes: III. Cem Concr Res 1973;3:689–700.
[45] Milestone NB. Hydration of tricalcium silicate in the presence of lignosulfonates, glucose, and sodium gluconate. J Am Ceram Soc 1979;62:321–4.
[46] Kakali G, Perraki T, Tsivilis S, Badogiannis E. Thermal treatment of kaolin: the effect of mineralogy on the pozzolanic activity. Appl Clay Sci 2001;20(1–2):73–80.